# Grid performance models using Design of Experiments (DoE) methods

**IEPC 2005-139**

*Presented at the 29th International Electric Propulsion Conference, Princeton University, October 31 – November 4, 2005*

Michael Tartz*, Jan H. Peters, Horst Neumann†

*Leibniz-Institute for Surface Modification, Leipzig, Germany*

**The Design of Experiments (DoE) approach is used to build models of beamlet parameters as the extracted beamlet current, beamlet divergence and the perveance limit in dependence on grid parameters and plasma density employing our well-approved beamlet simulation code. Appropriate polynomial degrees for the input parameters are determined which result in a mean deviation of the models from additional simulated test data of less than 4%. The derived models are obtained at a low computational effort and are helpful in designing and optimizing ion source extraction systems.**

## Nomenclature

| | | |
|---|---|---|
| $t_{scr}$ | = | screen grid thickness |
| $t_{acc}$ | = | accelerator grid thickness |
| $d$ | = | grid hole diameters (same for both grids) |
| $l_g$ | = | grid distance |
| $n$, $T_e$ | = | plasma density, electron temperature |
| $p(x_1,x_2,\ldots)$ | = | polynomial model (e.g. beamlet current, divergence, etc.) |
| $x_1$, $x_2$, ... | = | independent parameters in polynomial models (e.g. grid parameter as above) |
| $d_1$, $d_2$, ... | = | degree of each parameter $x_i$ |
| $c_{ijk...}$ | = | coefficients in polynomial (e.g. $c_{ijk}x_i^{di}x_j^{dj}x_k^{dk}$) |
| $w_1$, $w_2$,... | = | weights to calculate the coefficients $c_{ikj...}$ |

## I. Introduction

Gridded ion thrusters are high-efficient electrostatic ion beam sources used for spacecraft propulsion[1]. Successful missions proved their applicability for earth-orbit propulsion (e.g. NSSK) as well as for primary interplanetary propulsion[2,3,4,5].

Broad-beam ion sources, which basically use the same technologies, find increasingly application in high-demanding ultra-precise surface processing technologies[6] like smoothing, polishing of high-precision optical elements[7], structuring and thin film deposition[8].

Generally, in order to realize a technological application or a space flight mission a great deal of effort is invested to adapt the ion source to the particular requirements. Modelling of the ion beam generation opens a convenient way to study grid system properties and proved to be a helpful tool in tailoring the ion beam performance. At IOM a modu-

* michael.tartz@iom-leipzig.de

† horst.Neumann@iom-leipzig.de

lar modelling of the broad-beam properties[9] and grid erosion and lifetime[10] has been developed basing on the beamlet trajectory code IGUN[11], and extensively validated. Figure 1 shows as example the changing beamlet divergence with increasing plasma density and the occurrence of direct impingement when excessing the perveance limit.

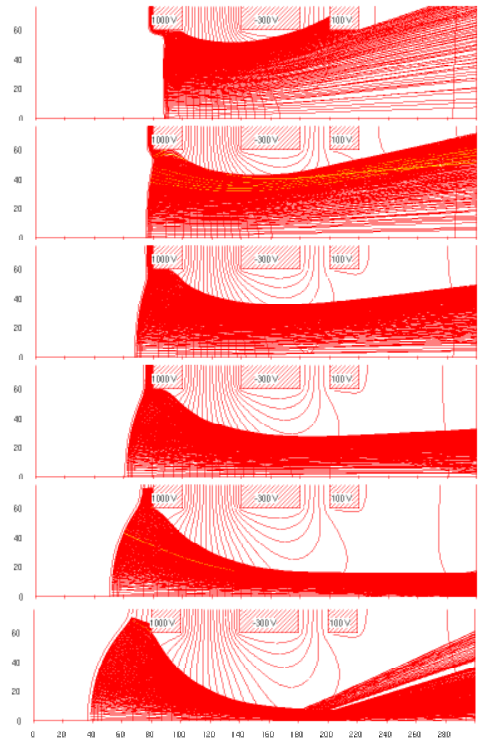

**Figure 1: Beamlets at increasing plasma density (upward) simulated with IGUN.**

For many technological applications the ion beam current density on the target and its homogeneity are the critical parameters. On the beamlet level the extracted beamlet current and the angular distribution of ion directions are relevant. The latter is characterized by the beamlet divergence defined as the half angle of the cone comprising 75% of the beamlet ions. In propulsion applications also the lifetime of the grid is important which is determined by the impact of charge-exchange ions on the grids, by the inset of electron backstreaming and the perveance limit. The optimization of an ion extraction system (e.g. towards low beam divergence or longer grid lifetime) is complicated by the large number of parameters (grid geometry, voltages, plasma parameters, mass flow properties), which influence the ion extraction and beam properties. Simulations usually yield the beamlet properties for a given parameter set only. In order to come to a more general grid design understanding, a very large number of simulations has to be performed varying all of the relevant parameters which leads to a vast quantity of data and reduces the clearness. Summarising this data in a model would make the changes of the beamlet properties easier to understand.

In this paper we describe an approach to a general model of the extracted beamlet properties in dependence on the geometrical grid and plasma parameters and voltages using the Design of Experiments (DoE) method. DoE is a systematic approach to investigate the relationship between input parameters (as listed above) affecting a process and the output of that process (e.g. beamlet current or divergence) by designing a series of structured experiments (one experiment means one simulation run here). The relation is approximated by a polynomial with individual degrees of each parameter. With DoE maximum information about the process can be obtained while minimizing the effort required.

Software has been developed which allows to take as many parameters into consideration as required. For each parameter the polynomial degree can be defined separately. The software creates the experimental plan, calls the beamlet simulations and builds up the model automatically. The precision can be checked by additional experiments. The outcome is a numerical model, which approximates the interrelation between the beamlet parameter (e.g. divergence) and all relevant input parameters.

In this paper we give a short introduction into the DoE approach and the DoE-software. First results of the models of beamlet current and divergence in dependence on some grid and plasma parameters are presented. A model giving the perveance limit in dependence on grid parameters is presented.

## II. The Design of Experiments (DoE) approach

Simple *Experimental designs* and *factorial plans* where developed in the first half of the last century by Fisher[12] and Box and Wilson[13]. They offered a way to estimate the dependence of a measured result $p$ on several parameters $x_i$ from a relatively small number of experiments and were mainly used to increase the efficiency of production processes. With the help of modern computer technology, the principles of their work can be used to develop more flexible models whose complexity is now mainly limited by the amount of available data.

A current implementation produces polynomials in $N$ parameters $x_1,x_2,...,x_N$ each to an individual degree $d_1,d_2,...,d_N$

$$p(x_1,x_2,\ldots,x_N)=\sum_{n_1,n_2,\ldots,n_N=0}^{d_1,d_2,\ldots,d_N} c_{n_1,n_2,\ldots,n_N}\prod_{m=0}^{N} x_m^{n_m}$$

The results of the calculations are the coefficients $c$. The degree $d_n$ of each parameter has to be chosen in advance.

Given the number, degree and range of the parameters, an *experimental design* can be created consisting of a list of experiments to perform (i.e. the points in the parameter space, where measurements are to be taken) and a *factorial plan* to calculate the coefficients from the measured experimental results. Usually, $d_n + 1$ equally distributed values are chosen in the range of each parameter $x_n$ and one experiment is performed for each possible combination $x_1,x_2,...,x_N$ of these values in each parameter. However, this choice is not mandatory as long as still at least $d_N+1$ different values are attained by each parameter and additional measurements can be included into the design, often improving the result.

The factorial plan can be (and was in earlier applications of DoE) expressed in form of a table containing a column for each term (and therefore each coefficient) of the target function and a row for each experimental measurement. The entries of each row of the table are the weights $w_n$ of a weighted sum by which the corresponding coefficient $c$ can be calculated from the measurements $y(x_1,x_2,...,x_N)$

$$c_{n_1,n_2,\ldots,n_N}=\frac{\sum w_n\cdot y(x_1,x_2,\ldots,x_N)}{\sum w_n\cdot\prod_{m=0}^{N} x_m^{n_m}}$$

The appropriate choice of weights $w_n$ is indicated by assuming the measurements $y(x_1,...,x_N)$ to be the values of a polynomial function of the actual form of the target-polynomial $p(x_1,...,x_N)$. So that the weighted sum takes the form

$$\begin{aligned}c_{n_1,n_2,\ldots,n_N}&=\frac{1}{W}\sum w_n\cdot\sum_{n_1,n_2,\ldots,n_N=0}^{d_1,d_2,\ldots,d_N} c_{n_1,n_2,\ldots,n_N}\prod_{m=0}^{N} x_m^{n_m}\\&=\frac{1}{W}\sum_{n_1,n_2,\ldots,n_N=0}^{d_1,d_2,\ldots,d_N} c_{n_1,n_2,\ldots,n_N}\sum w_n\cdot\prod_{m=0}^{N} x_m^{n_m}\end{aligned}$$

where equality is attained if all but one of the summands turns zero. Hence the weights for each coefficient can be found as the solution of a system of linear equations.

A program implementing the algorithms of DoE described above and interfacing the beamlet simulation software has been developed to automatically generate, execute and evaluate even more complex (>100 measurements on presently three parameters) experimental designs. The target function was supposed to describe the dependence of ion beamlet current and divergence on the plasma density, geometrical grid parameters and voltages. Comparison of the calculated model with a set of randomly chosen measurements (i.e. beamlet simulations) allows to evaluate the accuracy of the model.

## III. Models of beamlet properties

In order to determine the appropriate modelling degree of each input parameter, 2-parameter models of the beamlet current and divergence combining each geometrical grid parameter with the plasma density are build. The larger models comprising more parameters can be created with the estimated degrees assuming that there are no significant interrelations between the parameters. In order to estimate the precision of each model, for 500 additional measurement test points the deviation from the respective model results and the maximum and mean relative errors were calculated. For some models further comparison was done between model-derived dependencies and simulated ones. Table 1 gives the standard grid parameter values and the variation range within the model.

### A. Two-parameter models of extracted beamlet current

The extracted beamlet current is mainly a quadratic function of the hole diameter $d$, therefore a degree of 2 was chosen. The current increases almost linearly with the plasma density $n$, however, in the low-density region (up to

**Table 1: Geometrical parameters and voltages of the grid system used in the modelling**

| parameter | standard value | modelling range |
|---|---|---|
| screen grid thickness $t_{scr}$ | 0.5 mm | 0.2 … 1.0 mm |
| accelerator grid thickness $t_{acc}$ | 1.0 mm | - |
| grid hole diameters (same for both grids) $d$ | 1.6 mm | 1.0 … 3.0 mm |
| grid distance $l_g$ | 1.0 mm | 0.3 … 1.7 mm |
| screen grid voltage | 800 V | - |
| accelerator grid voltage | -300 V | - |
| operating gas | argon | - |
| plasma density $n$ ($T_e$=3eV) | - | $1*10^{10}$ … $4*10^{11}$ $cm^{-3}$ |

$1.5*10^{11}$ $cm^{-3}$) the simulated current is somewhat above the linear model (cf. figure 2). This is traced back to the movement of the plasma sheath with decreasing plasma density from inside the screen grid hole towards the plasma, which leads to an increasing effective emitting sheath area[14]. In order to describe this effect properly a higher degree was chosen for $n$. The minimum mean relative deviation of the additional test point currents from the model is achieved at degree 5 for $n$ and amounts 1.1%. Figure 2 shows the good agreement between experimental (i.e. simulated) and modeled beamlet current obtained with a $d^2n^5$ model. The plot of the relative deviation between modeled and experimental beamlet currents in dependence on plasma density and hole diameter in figure 4 shows that the largest deviation occurs at very low plasma densities and small holes. However, depending on the aim of the model a lower degree of $n$ might be sufficient where, as example with $d^2n^3$ model, model and experimental values differ at a mean deviation of 4.7% and an maximum of 15% at lower plasma densities and small hole diameters.

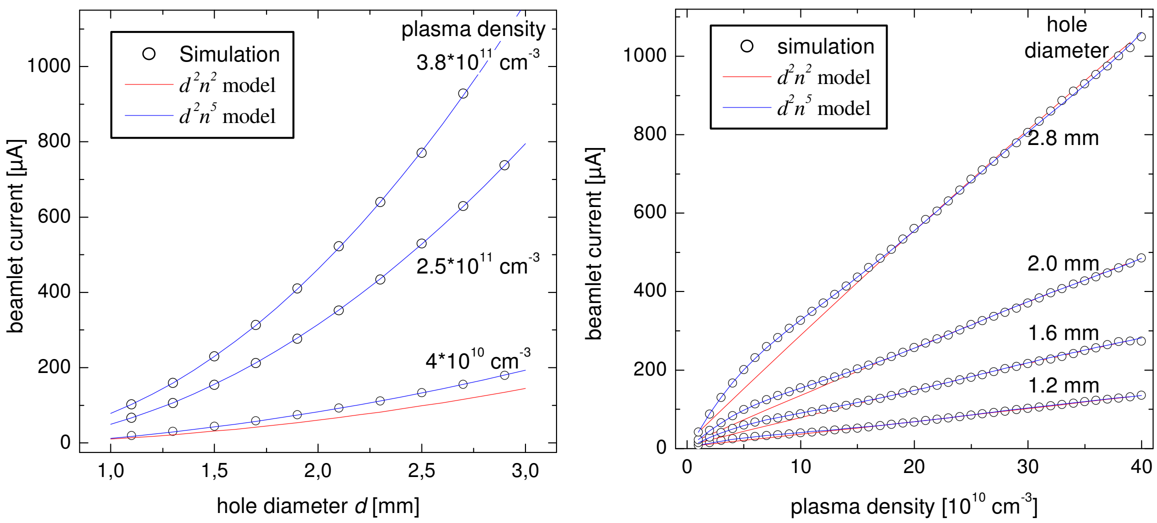


**Figure 2: Comparison of beamlet currents derived from model $d^2n^5$ with simulated values; right: dependence on plasma density, left: dependence on hole diameter (all other parameter as in table 1).**

An increased thickness of the screen grid $t_{scr}$ reduces the extracted beamlet current approximately according to $1/t_{scr}$. To describe this dependence with a polynomial properly a higher degree of $t_{scr}$ has to be chosen, a good agreement was achieved with $t_{scr}^4$. Again, at lower plasma densities the current shows the same behavior as discussed above, therefore it seems obvious to apply the same functional degree as above. Consequently, a $t_{scr}^4n^5$ model yielded a good agreement with the simulated dependencies with a mean deviation of 2.1%. The largest deviations occur in the lower plasma density region.

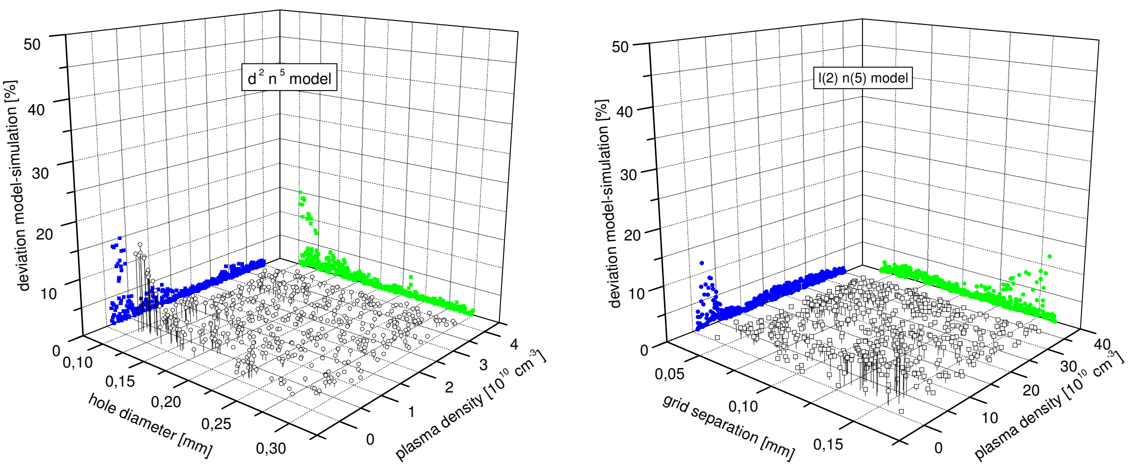


**Figure 3: Relative deviation between modeled and experimental beamlet currents (projections over *n* and *d* shown), left: d-n-model, right: $l_g$-n-model.**

Increasing the grid separation $l_g$ has a similar effect on the current as the screen grid thickness. However, it was found that a $l_g^2 n^5$ model gives a good approximation of the simulated dependencies (figure 3). The mean relative deviation amounts 1.1% at a maximum deviation of 11% found at low plasma densities and large grid separations (cf. right plot in figure 4).

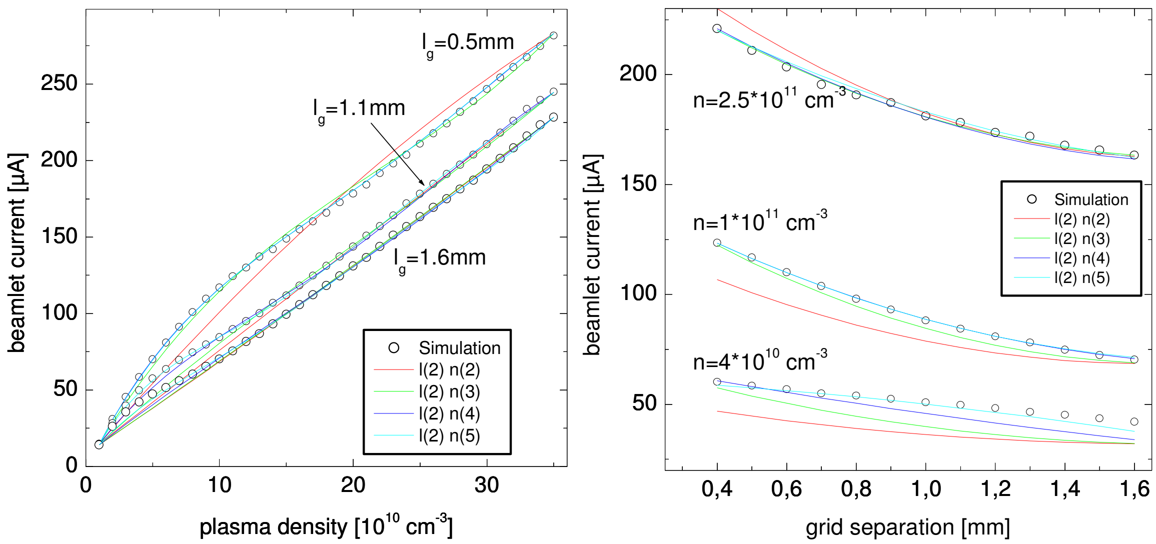


**Figure 4: Comparison of beamlet currents derived from model $l_g^2 n^5$ with simulated values; right: dependence on plasma density, left: dependence on hole diameter (all other parameter as in table 1).**

## B. Two-parameter models of beamlet divergence

The dependence of the beamlet divergence on all of these parameters is more complicated than that of the current because of the occurrence of a divergence minimum[15]. Furthermore, inset of direct impingement on the accelerator grid affects the beamlet divergence. The parameter variation range was chosen so that direct impingement occurs only at the periphery and is therefore not particularly treated here.

Figure 6 compares the simulated dependence of the beamlet divergence on the hole diameter *d* and plasma density *n* with the respective model results. The agreement improves with increasing degree of *n*. In order to describe the di-

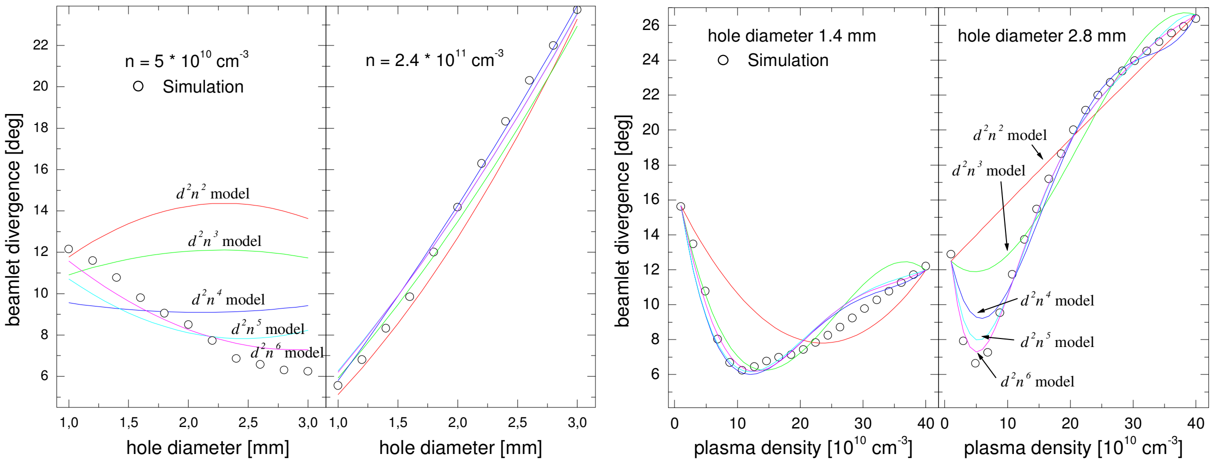


**Figure 5: Beamlet divergence in dependence on hole diameter (left) and plasma density (right) derived from various $d^i n^k$ models in comparison with simulated values (all other parameter as in table 1).**

vergence minimum properly (usually located in the low plasma density region) a degree of at least 5 for the plasma density is necessary (see bottom of figure 2). An increase of the degree of $d$ brings no further significant enhancement. The mean deviation of the $d^2n^5$ divergence model is 3.9% and 3.7% for the $d^2n^6$ model. The strongest deviation is found at lower plasma densities and larger hole diameters.

The dependence of the divergence on the grid separation is best described by a $l_g^3n^5$ model resulting in a mean deviation of 2.8%. The screen grid thickness is to be modelled as $t_{scr}^2n^5$ to yield a minimum mean deviation of 3.2% (see figure 5).

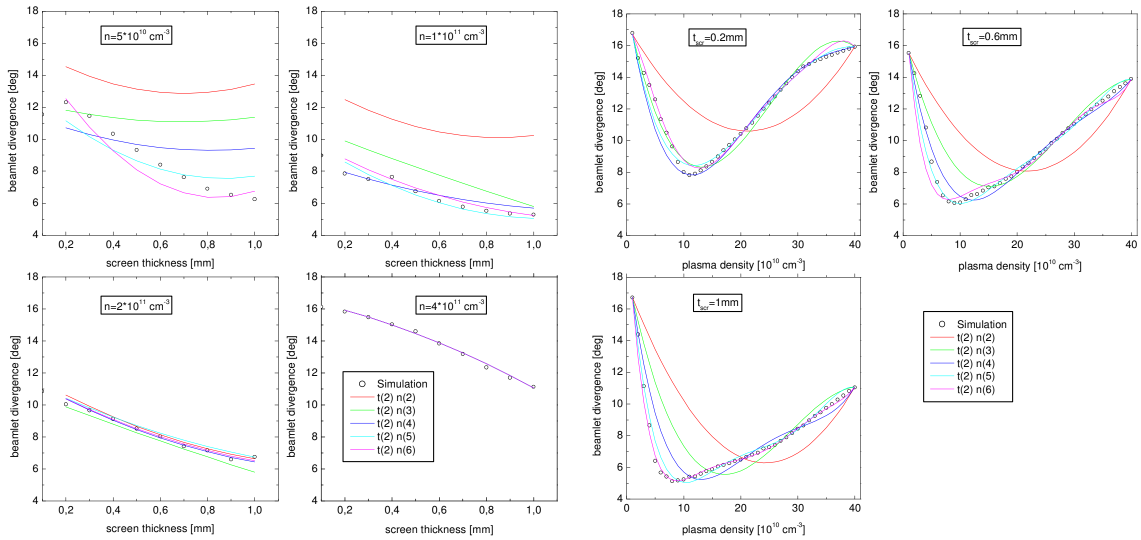


**Figure 6: Beamlet divergence in dependence on screen grid thickness (left) and plasma density (right) derived from various $t^i n^k$ models in comparison with simulated values (all other parameter as in table 1).**

Figure 7 shows the model divergence plot in dependence on grid hole diameter and plasma density illustrating the good agreement with the simulated one. The main deviations can be seen at low plasma densities and large grid holes as mentioned above. Such plots are used to adapt the grid geometry to application requirements, e.g. to low divergence, accounting for an inhomogeneous plasma density distribution. Whereas the left plot was obtained from 400 simulations, the right plot is calculated with the model, which was obtained from 18 simulations only.

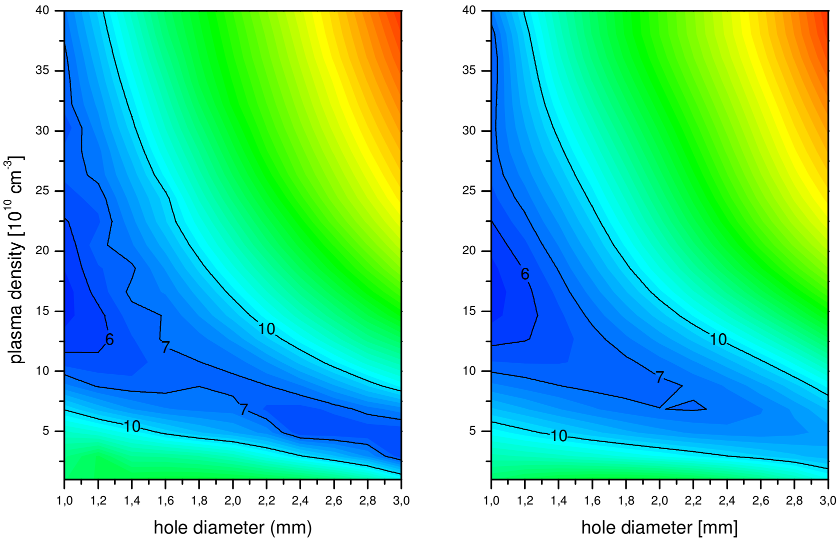


**Figure 7: The divergence in dependence on grid hole diameter and plasma density, left: simulation, right: $d^2n^5$ model.**

### C. Two-parameter model of the perveance limit

The perveance limit gives the plasma density value (or the perveance value) where the direct impingement on the accelerator grid sets in. It is mandatory in designing grid systems to stay below this limit even though an inhomogeneous plasma density distribution is taken into consideration.

Figure 8 shows the model of the perveance limit (plasma density) in dependence on the screen grid thickness and the grid separation. As expected, the perveance limit decreases with growing grid distance and decreasing screen grid thickness. The mean deviation between the $t^2l^2$ model and additional test values is 1.7% with a maximum deviation of 5.2% occurring at larger grid distances.

Figure 9 shows the perveance limit model in dependence on the screen grid thickness and grid hole diameters. With growing hole diameters the perveance limit decreases. The mean deviation between the $t^2d^2$ model and additional test values is 1.3% with a maximum deviation of 6%.

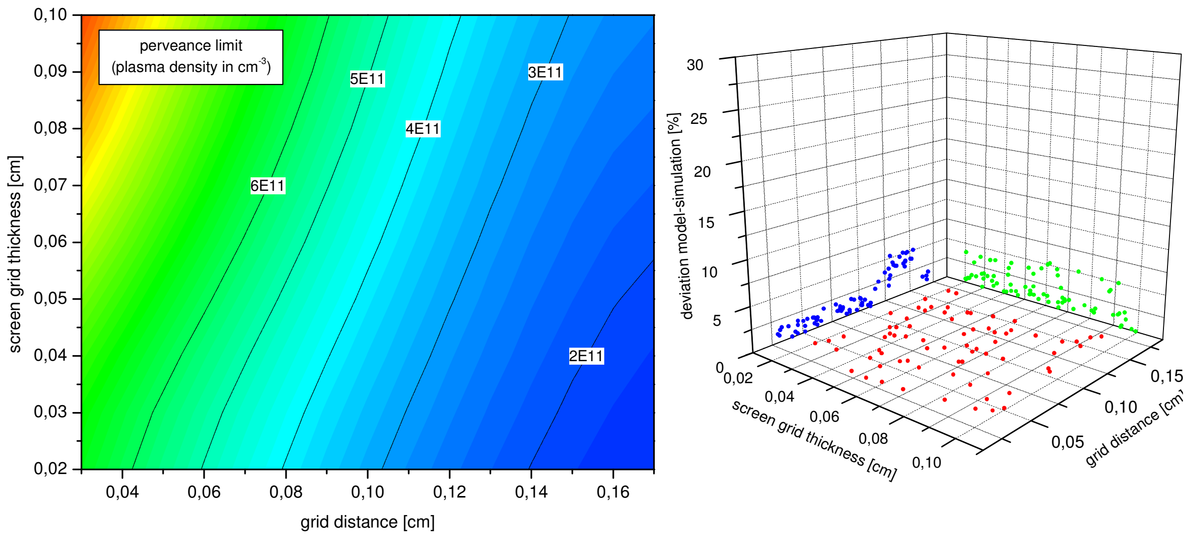


**Figure 8: Left: Model $t^2l^2$ of the perveance limit in dependence on screen grid thickness and grid distance (all other parameters as in table 1). Right: Relative Deviation between additional test values and model.**

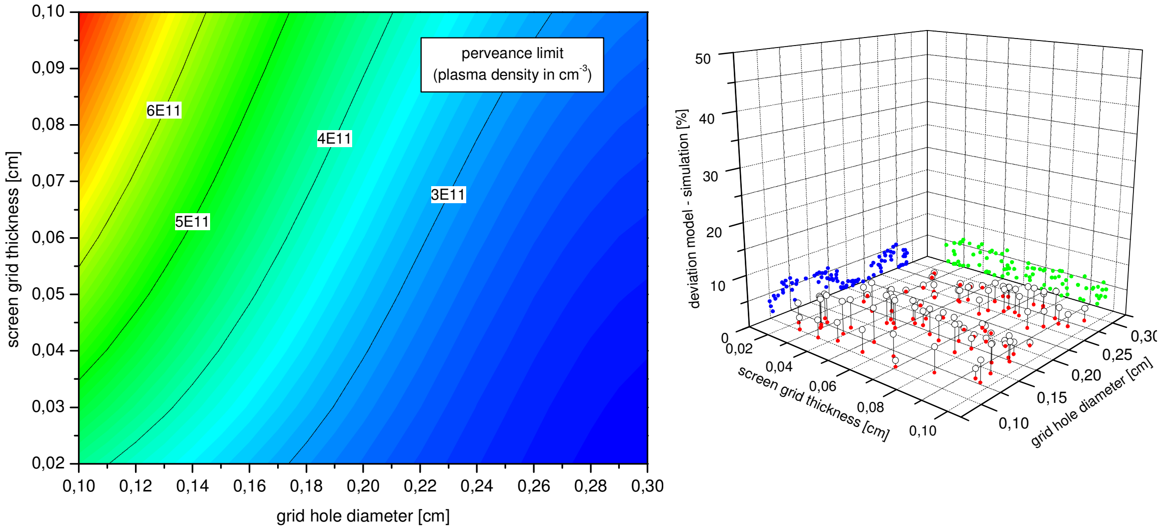


**Figure 9: Left: Model $t^2d^2$ of the perveance limit in dependence on screen grid thickness and grid hole diameter (all other parameters as in table 1). Right: Relative Deviation between additional test values and model.**

For a given maximum plasma density in the particular device, the grid design has to stay on the left side of the equi-density lines in the model plots in figures 8 and 9 in order to avoid direct impingement on the accelerator grid.

### D. Discussion

The two-parameter models proved to describe the simulated dependencies very well and can be used for optimization of grid systems, e.g. to find the minimum divergence conditions or the conditions for a required divergence value. As compared to the direct creation of such dependencies by a very large number of single simulation runs the effort is significantly reduced by using the DoE approach. The here often-derived $x^2y^5$ model, as example, requires only 18 supporting points to be simulated notwithstanding the rather high-degree of the model.

If such models have to be build for other parameter sets (i.e. other values as in table 1) we assume that the derived model structures will also be applicable in these cases and the optimal degrees of the variables will not differ from that obtained here.

While the value of the model seems to depend strongly on the degree of the parameters, this choice currently depends either on prior knowledge or on the evaluation of the models using a large number of further measurements. Algorithms to evaluate the quality of the model by a small number of additional measurements would be helpful.

The inclusion of additional measurements into the experimental design may improve the accuracy of the model. Heuristics to choose appropriate supporting points (e.g. near extreme values) should be evaluated. Furthermore, the inclusion of non-polynomial target-functions adapted to the expected dependencies seems possible and could allow to reduce the number of required experiments. This will probably overcome the deviations occurring in the lower plasma density region where the beamlet divergence minima are located and which is currently modeled at higher degrees ($n^5$) satisfactory. These topics will be addressed in the near future.

## IV. Conclusion

Polynomial models of the extracted beamlet current, beamlet divergence and perveance limit of a 2 grid extraction system have been determined in dependence on geometrical grid parameters like hole diameters, screen grid thickness and grid distance and the plasma density using a validated beamlet simulation code. The Design of Experiments (DoE) approach gives an algorithm to obtain the models with a reduced computational effort by using a few supporting values only. A dedicated software was developed to perform this process.

The resulting two-parameter models include the plasma density at a degree of 5 and the geometrical parameters at lower degrees. Lower-degree models best describe the perveance limit. The models agreed very well with the simulated dependencies at a mean relative deviation of less than 4%.

The work will be continued to include more parameters in the models making them more generally. Such multi-parameter models are useful in designing grid systems. They help to come to a quick understanding what happens if one changes a grid parameter.

Some topics to improve the accuracy and effectivity of the model were addressed which will be studied in future work.

## References


[1] P. J. Wilbur, V. K. Rawlin, J. R. Beattie, J. Propulsion Power 14 (1998) 708.

[2] J. E. Polk, R. Y. Kakuda, J. R. Anderson, J. R. Brophy, V. K. Rawlin, M. J. Patterson, J. Sovey, J. Hamley, *Validation of the NSTAR ion propulsion system on the Deep Space One mission - Overview and initial results*, AIAA-1999-2274, 35$^{th}$ Joint Propulsion Conf., Los Angeles, CA, June 20-24, 1999.

[3] R. Killinger, R. Kukies, M. Surauer, H. Gray, G. Saccoccia, *Final Report on the ARTEMIS Salvage Mission Using Electric Propulsion*, AIAA-2003-4546 39th Joint Propulsion Conf., Huntsville, AL, July 20-23, 2003.

[4] J. Brophy, M. Marcucci, J. Gates, C. Garner, B. Nakazono, G. Ganapathi, *Status of the Dawn Ion Propulsion System*, AIAA-2004-3433, 40th Joint Propulsion Conf., Fort Lauderdale, FL, July 11-14, 2004.

[5] H. Kuninaka, Y. Shimizu, T. Yamada, I. Funaki, K. Nishiyama, *Flight Report During Two Years on HAYABUSA Explorer Propelled by Microwave Discharge Ion Engines*, AIAA-2005-3673, 41$^{st}$ Joint Propulsion Conf., Tucson, AZ, July 10-13, 2005.

[6] B. Wolf, *Handbook of ion sources*, CRC Press, Boca Raton, 1995.

[7] A. Schindler, T. Hänsel, F. Frost, G. Böhm, W. Frank, A. Nickel, T. Arnold, R. Schwabe, S. Gürtler, S. Görsch, B. Rauschenbach, *Modern Methods of Highly Precise Figuring and Polishing*, Glass Science and Technology 78 (Suppl. C) (2005) 111.

[8] T. Chassé, H. Neumann, B. Ocker, M. Scherer, W. Frank, F. Frost, D. Hirsch, A. Schindler, M. Lorenz, G. Otto, M. Zeuner, B. Rauschenbach, *Mo/Si-Multilayers for EUV-Lithography by Ion Beam Assisted Deposition*, Vacuum 71 (2003) 407.

[9] M. Tartz, R. Deltschew, E. Hartmann, H. Neumann, *Effect of the plasma inhomogeneity on grid performance,* Surf. Coat. Technol. 142-144 (2001) 34.

[10] M. Tartz, E. Hartmann, H. Neumann, *Evolution of extraction grid erosion with operation time,* Paper AIAA-2004-3787, 40. Joint Propulsion Conf., Ft. Lauderdale, 11.-14.7. 2004.

[11] R. Becker, W. B. Herrmannsfeldt, Rev. Sci. Instrum. 63 (1992) 2756.

[12] R. A. Fisher, *The Design of Experiments*, London – Edinburgh, Oliver and Boyd 1966.

[13] G. E. P. Box, K. B. Wilson, *On the experimental attainment of optimum conditions*, J. Royal Statistical Soc., Ser. **B13** (1951), 1-45.

[14] M. Tartz, E. Hartmann, F. Scholze, H. Neumann, *Modelling of broad beam ion sources,* Rev. Sci. Instr. 69 (1998) 1147.

[15] T. S. Green, Rep. Progr. Phys. 37 (1974) 1257-1344.